Equine Herpesvirus 1 (EHV-1) Glycoprotein M: Effect of Deletions of Transmembrane Domains

Christian Seyboldt,* Harald Granzow,† and Nikolaus Osterrieder*,[1]

Institutes of *Molecular Biology and †Infectology, Friedrich-Loeffler-Institutes, Federal Research Centre for Virus Diseases of Animals,
D-17498 Insel Riems, Germany

Equine herpesvirus 1 (EHV-1) recombinants that carry either a deletion of glycoprotein M (gM) or express mutant forms of gM were constructed. The recombinants were derived from strain Kentucky A (KyA), which also lacks genes encoding gE and gI. Plaques on RK13 cells induced by the gM-negative KyA were reduced in size by 80%, but plaque sizes were restored to wild-type levels on gM-expressing cells. Electron microscopic studies revealed a massive defect in virus release after the deletion of gM in the gE- and gI-negative KyA, which was caused by a block in secondary envelopment of virions at Golgi vesicles. Recombinant KyA expressing mutant gM with deletions of predicted transmembrane domains was generated and characterized. It was shown that mutant gM was expressed and formed dimeric and oligomeric structures. However, subcellular localization of mutant gM proteins differed from that of wild-type gM. Mutant glycoproteins were not transported to the Golgi network and consequently were not incorporated into the envelope of extracellular virions. Also, a small plaque phenotype of mutant viruses that was indistinguishable from that of the gM-negative KyA was observed. Plaque sizes of mutant viruses were restored to wild-type levels by plating onto RK13 cells constitutively expressing full-length EHV-1 gM, indicating that mutant proteins did not exert a transdominant negative effect on wild-type gM. © 2000 Academic Press

INTRODUCTION

Equine herpesvirus 1 (EHV-1) is a member of the *Alphaherpesvirinae* and is assigned to the genus *Varicellovirus* (O'Callaghan and Osterrieder, 1999). EHV-1 causes abortion in pregnant mares, rhinopneumonitis, and neurological disorders, the latter being irregularly associated with infection (Allen and Bryans, 1986). Envelope glycoproteins of EHV-1 are designated according to their homologs of the prototype member of the *Alphaherpesvirinae*, herpes simplex virus 1 (HSV-1). During the past years, a better understanding of the properties and functions of EHV-1 glycoproteins has been obtained. EHV-1 glycoproteins (g) B and D are essential virus components that function in virus penetration, virus release, and cell-to-cell spread of infectivity (Neubauer *et al.,* 1998; Csellner *et al.,* 1999). EHV-1 gC is responsible for interaction of the virion with glycosaminoglycans of the target cell surface and plays a role in virus penetration and egress (Osterrieder, 1999a). Glycoproteins E and I are nonessential for virus growth but are involved in cell-to-cell spread (Flowers and O'Callaghan, 1992; Matsumura *et al.,* 1996, 1998). Although the expression of other EHV-1 glycoproteins (gG, gH, gK, and gL) has been demonstrated, nothing is known about their functions in

the replicative cycle (Colle *et al.,* 1992; Crabb *et al.,* 1992; Stokes *et al.,* 1996; Zhao *et al.,* 1992).

Glycoprotein M is a nonessential glycoprotein that is conserved throughout all herpesviral subfamilies (reviewed in Jöns *et al.,* 1998). EHV-1 gM, like its counterparts in other herpesviruses, represents a multiply hydrophobic class III membrane protein that contains eight putative transmembrane domains (Osterrieder *et al.,* 1996; Pilling *et al.,* 1994; Telford *et al.,* 1992). EHV-1 gM is translated into an M_r 44,000 polypeptide that is cotranslationally glycosylated to an M_r 46,000–48,000 glycoprotein. In the *trans*-Golgi network (TGN) and in extracellular virions, EHV-1 gM is present as an M_r 50,000–55,000 mature glycoprotein that forms dimers and oligomers in both infected cells and purified virions (Osterrieder *et al.,* 1996, 1997). The deletion of gM in the EHV-1 wild-type strain RacL11 leads to a reduction in plaque size of ~50% compared with that of wild-type RacL11 and to an ~50- to 100-fold reduction in extracellular virus titers, whereas the deletion of gM in the *syn* EHV-1 strain RacH has virtually no influence on plaque size or production of infectious progeny (Neubauer *et al.,* 1997a; Osterrieder *et al.,* 1996). It has been shown that pseudorabies (PrV) gM lacks a cleavable N-terminal signal sequence (Dijkstra *et al.,* 1996, 1997a,b) and that the C-terminus of mature PrV and EHV-1 gM is located on the cytoplasmic side of the plasma membrane (Dijkstra *et al.,* 1997b; Osterrieder *et al.,* 1996, 1997). Recently, gM has been shown to be disulfide-linked to the UL49.5 product in PrV and bovine herpesvirus 1 (BHV-1). Similarly, Epstein–Barr

[1] To whom reprint requests should be addressed at Federal Research Centre for Virus Diseases of Animals, Boddenblick 5a, D-17498 Insel Riems, Germany. Fax: 49-38351-7151. E-mail: klaus.osterrieder@rie.bfav.de.
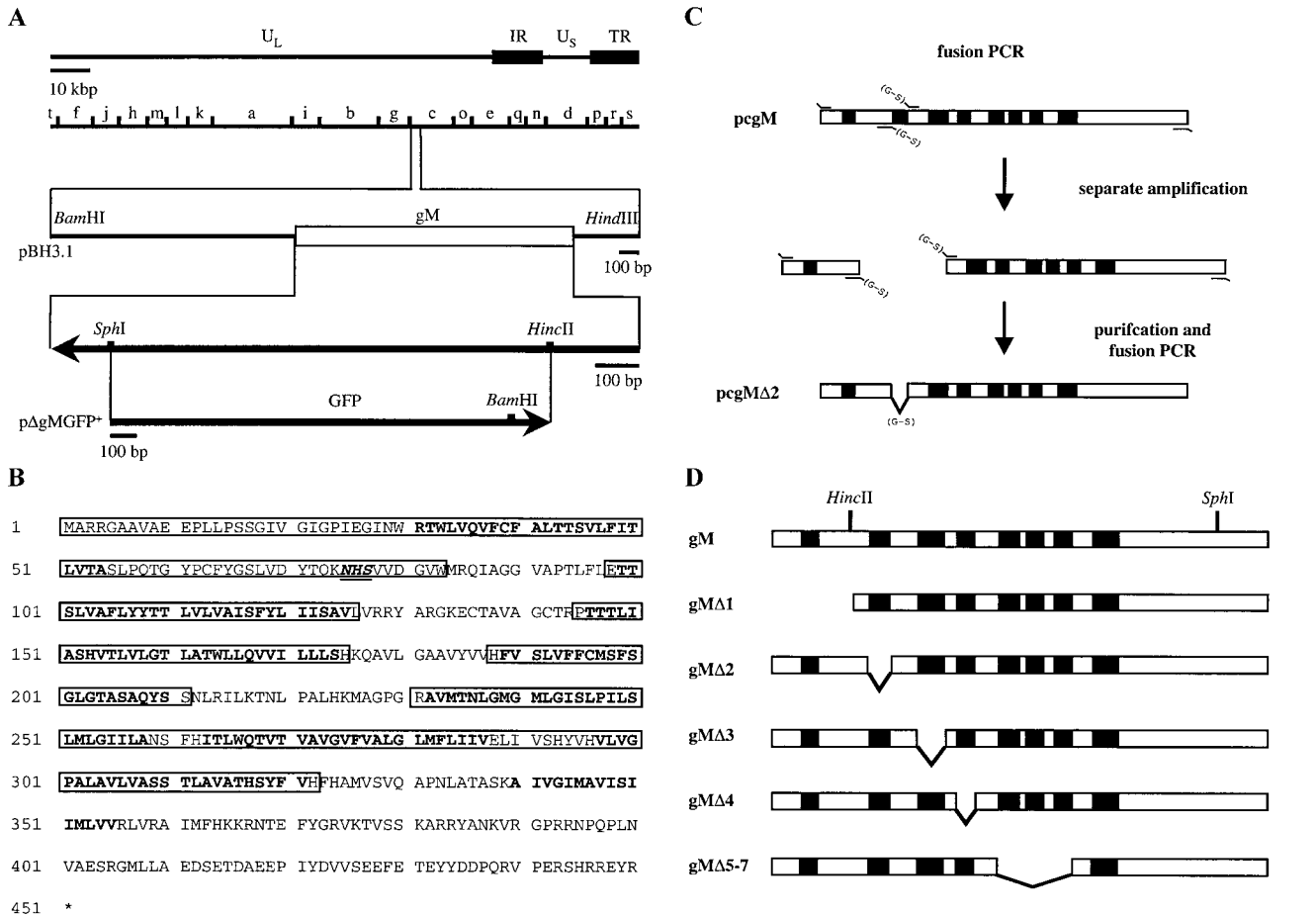
A

B

```
  1   MARRGAAVAE EPLLPSSGIV GIGPIEGINW RTWLVQVFCF ALTTSVLFIT

 51   LVTASLPQTG YPCFYGSLVD YTQKNHSVVD GVWMRQIAGG VAPTLFIETT

101   SLVAFLYYTT LVLVAISFYL IISAVIVRRY ARGKECTAVA GCTRPTTTLI

151   ASHVTLVLGT LATWLLQVVI LLLSHKQAVL GAAVYVVHFV SLVFFCMSFS

201   GLGTASAQYS SNLRILKTNL PALHKMAGPG RAVMTNLGMG MLGISLPILS

251   LMLGIILANS FHITLWQTVT VAVGVFVALG LMFLIIVELI VSHYVHVLVG

301   PALAVLVASS TLAVATHSYF VHFHAMVSVQ APNLATASKA IVGIMAVISI

351   IMLVVRLVRA IMFHKKRNTE FYGRVKTVSS KARRYANKVR GPRRNPQPLN

401   VAESRGMLLA EDSETDAEEP IYDVVSEEFE TEYYDDPQRV PERSHRREYR

451   *
```

C

D

FIG. 1. (A) *Bam*HI restriction map of the EHV-1 genome and recombinant plasmids. Diagram of the EHV-1 genome consisting of the unique long (U$_L$) and short (U$_S$) regions, with the position of the inverted repeats (IR and TR). Plasmid pBH3.1 contains gM and adjacent sequences. The gM ORF with the relevant restriction sites used for cloning is given as an open box. A 1010-bp *Hinc*II–*Sph*I fragment was deleted and replaced by a 1641-bp EGFP expression cassette (Clontech) for generation of gM-negative KyA (KyAΔgM). (B) Amino acid sequence of gM: bold letters indicate predicted transmembrane domains, and the consensus N-glycosylation site (N-H-S) is underlined. Amino acids deleted in mutant gM genes are boxed. (C) Schematic diagram of the fusion PCR to generate mutant gM genes (details are given in the text). (D) Illustration of the generated gM mutants: black boxes indicate sequences encoding predicted transmembrane domains, and the restriction sites used for insertion of mutant gM genes (*Hinc*II and *Sph*I) are given.

virus (EBV) gM and the UL49.5 product, which is also referred to as gN in PrV and EBV, form hetero-oligomers (Jöns *et al.,* 1998; Lake *et al.,* 1998; Wu *et al.,* 1998). Based on its structure, the possible formation of a gM ion channel has been discussed; however, EHV-1 gM by itself does not constitute an ion channel as assayed by transient transfection in *Xenopus laevis* oocytes (Osterrieder *et al.,* 1997). The functional implications of the interaction between gM and itself and between gM and the UL49.5 protein (gN) are not well understood, nor is the function of individual gM domains.

The aim of this study was to systematically investigate the impact of a simultaneous deletion of gE, gI, and gM and that of deletions of predicted transmembrane domains of EHV-1 gM. By using a fusion polymerase chain reaction (PCR) protocol, mutant gM genes expressing proteins with deletions of individual transmembrane domains were generated and inserted into the viral ge-

nome instead of wild-type gM sequences. Biochemical and functional analyses demonstrated that mutant gM were expressed on infection but lacked wild-type gM function. However, mutant gM did not exert a transdominant negative effect on wild-type gM, which was demonstrated by functional assays on cells providing wild-type or mutant gM *in trans*.

RESULTS

Construction and characterization of a gM-negative KyA virus

A gM-negative KyA was produced by cotransfection of the gM-expressing cell line RKgM with KyA DNA and plasmid pΔgMGFP+ (Fig. 1A). Virus progeny from the transfection that appeared green under the fluorescent microscope was harvested after plating onto RKgM cells.
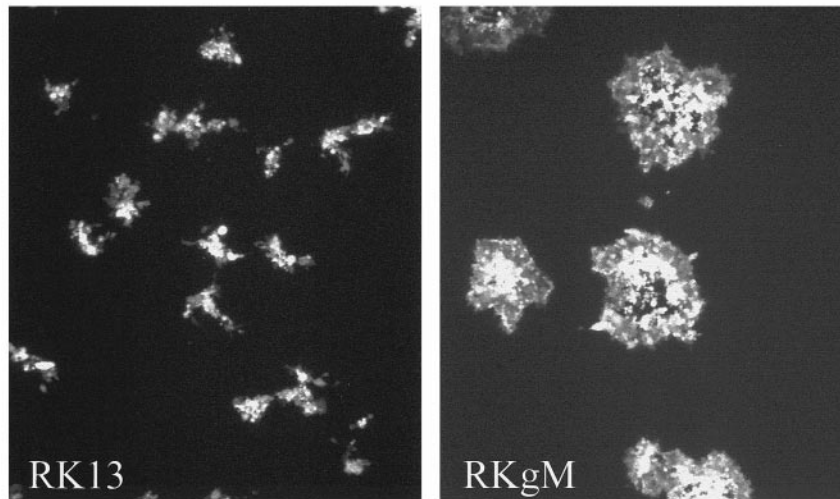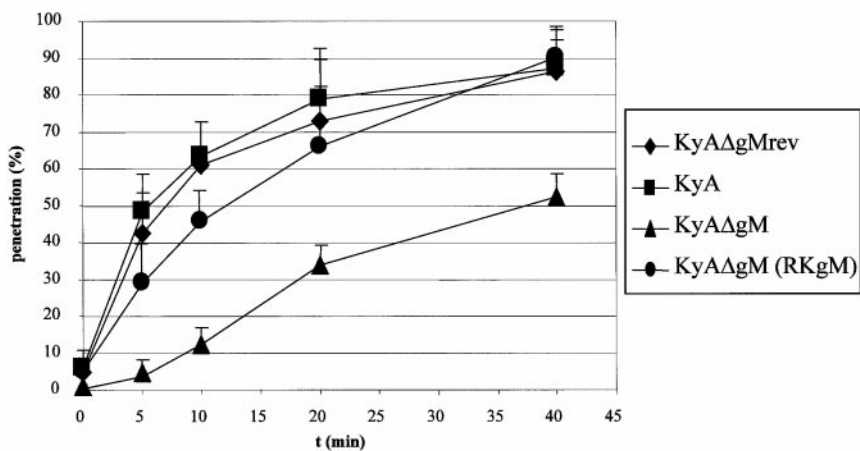
FIG. 2. (A) Digitally processed images of plaques induced by KyAΔgM on RK13 cells and on transcomplementing RKgM cells analyzed by immunofluorescence microscopy. KyAΔgM-induced plaques on RK13 cells were reduced in size to ~20% compared with plaques on gM-expressing cells. Magnification, 250×. (B) Penetration kinetics of KyA, gM-negative KyAΔgM grown on either RK13 or gM-complementing RKgM cells, and rescuant virus KyAΔgMrev. The graph shows the percentage of virus protected from acid treatment at the indicated times after adsorption and temperature shift to 37°C from three independent experiments (see Materials and Methods). Error bars indicate standard deviations.

Green fluorescing virus plaques were purified to homogeneity. Southern blot (data not shown) and Western blot analyses as well as indirect immunofluorescence (IIF) using anti-gM monoclonal antibody (MAb) P1/B6 A8 demonstrated that the gM open reading frame (ORF) was deleted in KyAΔgM and that no expression of gM was detectable (see Figs. 5B and 6). Plating of KyAΔgM onto RK13 cells revealed a severe impairment of this virus in cell-to-cell spread such that the sizes of KyAΔgM plaques were reduced to ~20% of the size of plaques induced by parental KyA (Fig. 2A). This defect in cell-to-cell spread could be completely reversed when KyAΔgM was plated onto gM-expressing RKgM cells (Fig. 2A). From the massive reduction in plaque sizes and the results of the titration experiments (see later), it was concluded that the deletion of gE, gI, and gM in EHV-1, as

reported for PrV triple-deletion mutants, led to a significant impairment in cell-to-cell spread that was much more pronounced than that observed after the deletion of gM alone, where a reduction in plaque size of only up to 50% was observed (Neubauer et al., 1997b; Osterrieder et al., 1996). In addition, penetration kinetics of KyAΔgM grown on RK13 or RKgM cells were determined and compared with those of parental KyA (Fig. 2B). As reported previously for an RacL11 gM-negative mutant (Osterrieder et al., 1996), KyAΔgM entered target cells more slowly than either parental KyA or KyAΔgM that was phenotypically complemented by propagation on RKgM cells (Fig. 2B). The results of the penetration kinetics of KyAΔgM confirmed the involvement of gM in virus entry.
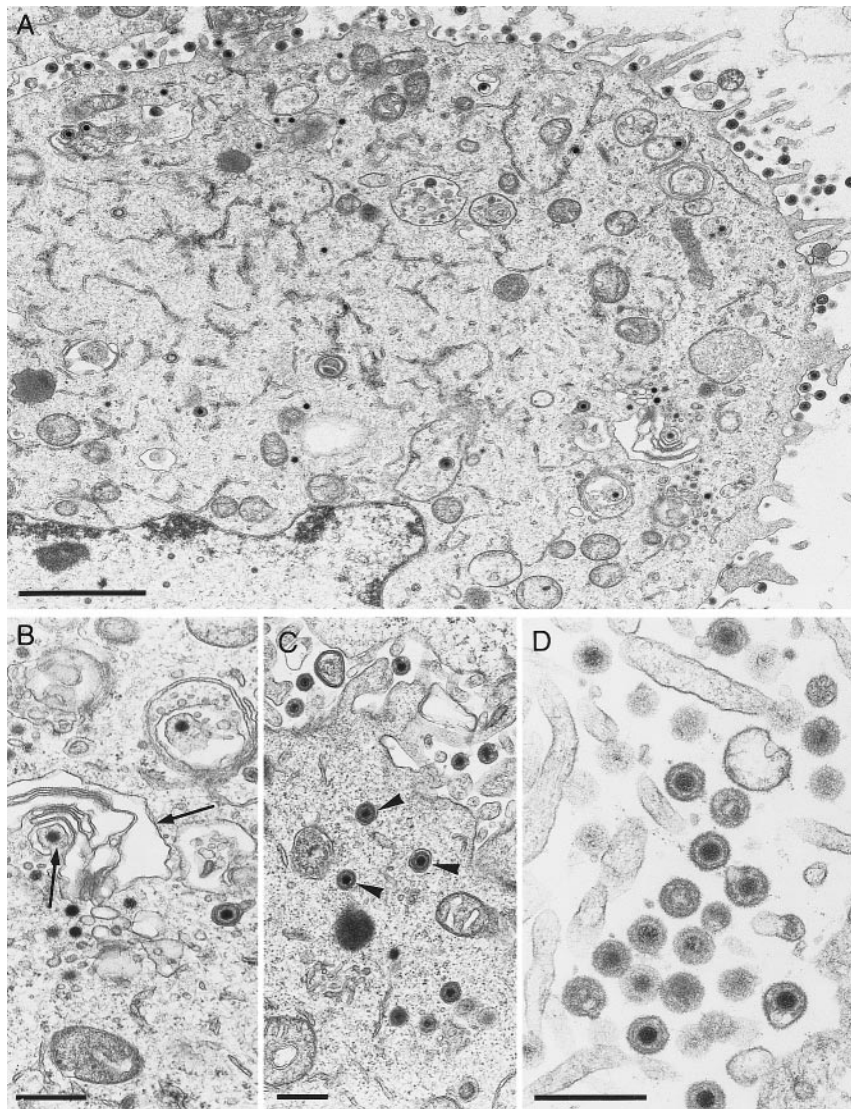
To further examine the reason for the massive im-

FIG. 3. Electron micrographs of RK13 cells infected with EHV-1 strain KyA at 18 h p.i. (A) Overview of a section of an infected cell. Various stages of EHV-1 morphogenesis can be seen. Note the large number of released virions at the cell surface. (B) Secondary envelopment of cytoplasmic virions at Golgi membranes (arrows). (C) Double-enveloped mature virions were detected in secretory Golgi vesicles (arrowheads). (D) Higher magnification of virions present in the extracellular space. Bar represents 2 μm (A) or 500 nm (B–D).

pairment of virus egress and cell-to-cell spread of gM-negative KyA, ultrastructural studies were performed. These studies revealed that replication of EHV-1 strain KyA (an overview is shown in Fig. 3A) follows the same morphogenetic steps that were previously described for PrV (Granzow *et al.,* 1997) (i.e., after primary envelopment by budding at the nuclear membrane, nucleocapsids appeared to be deenveloped in the cytoplasm and to receive their final envelope by budding at membranes of the Golgi network) (Fig. 3B). Virus-containing vesicles (Fig. 3C) released their content by fusion at the cell membrane, and a great number of virions were visible in the extracellular space (Figs. 3A and 3D). In contrast, gM-negative KyAΔgM exhibited a pronounced defect in secondary envelopment at Golgi membranes, although capsid

formation in infected-cell nuclei, primary budding at the nuclear membrane, and deenvelopment did not appear to be different from the situation observed in KyA-infected cells (data not shown). Budding of nucleocapsids at membranes of the Golgi network was observed only very rarely, and deenveloped nucleocapsids accumulated in the Golgi region (Figs. 4A and 4B). Higher magnification of the accumulated nucleocapsids revealed a clearly detectable rim of fuzzy material, presumably tegument proteins, around cytoplasmic nucleocapsids (Fig. 4C). Virions juxtaposed to the cell surface that appeared to be the result of previously lysed virus-infected cells were observed only sporadically (Fig. 4A). Taken together, the electron microscopic studies demonstrated that the impairment of KyAΔgM in cell-to-cell spread was caused
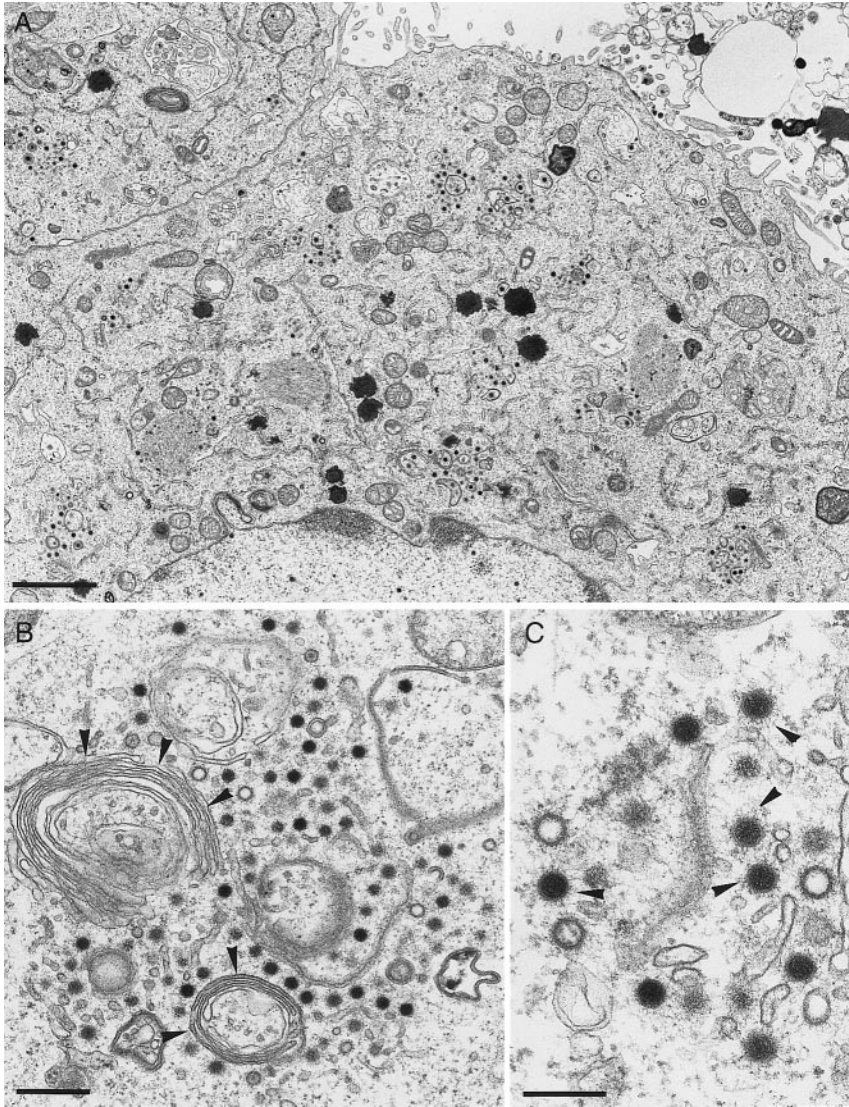
FIG. 4. Electron micrographs of RK13 cells infected with KyAΔgM at 18 h p.i. (A) Overview of a section of an infected cell. Nucleocapsids in the nucleus and the cytoplasm are visible. However, only few virions in secretory vesicles or virions in the extracellular space can be detected. (B) Cytoplasmic nucleocapsids were released from infected-cell nuclei and accumulated in the vicinity of Golgi membranes (arrowheads). (C) Higher magnification demonstrated fuzzy material, probably representing tegument proteins, around cytoplasmic nucleocapsids (arrowheads). Bar represents 2 μm (A), 500 nm (B), or 250 nm (C).

by a defect in secondary envelopment of virions at Golgi membranes.

Analysis of cell lines expressing mutant gM

A total of five mutant gM genes were constructed by (fusion) PCR and cloned into eukaryotic expression vector pcDNA3 (Figs. 1C and 1D). Mutant ORF gMΔ1 starts with the second *in-frame* methionine codon at position 83 and consequently lacks the first transmembrane domain and the consensus *N*-glycosylation site (Figs. 1B and 1D). In mutant genes gMΔ2, gMΔ3, gMΔ4, and gMΔ5–7, the second, third, fourth, or fifth to seventh transmembrane domain, respectively, was replaced by a (Gly-Ser)$_4$ linker (Table 1 and Figs. 1B and 1D). Recom-

binant plasmids pcgMΔ1, pcgMΔ2, pcgMΔ3, pcgMΔ4, and pcgMΔ5–7 were transfected into RK13 cells, and stable cell lines were established that constitutively expressed the respective mutant gM polypeptides. Cell lines were analyzed by IIF followed by confocal laser scan microscopy and Western blotting using anti-gM MAb P1/B6 A8 or the gM-specific polyclonal pQEgM serum raised in a rabbit. Stable expression could be demonstrated for each of the mutant proteins by IIF. A mainly punctate pattern with a strong reactivity at nuclear rims was observed, and the distribution of mutant gM molecules was indistinguishable from that of full-length gM expressed in RKgM cells (data not shown). Stable expression was also confirmed by Western blot

TABLE 1

Primers Used for Construction of Mutant gM Genes

Name	Position[a]	Sequence[a]
start	94471 (+)	5'-atcggaattcATGGCACGACGGGGAGC-3'
stop	93119 (−)	5'-acgtctgcagttaCTATCGGTACTCCCGGCG-3'
del1for	94223 (+)	5'-caggatccATGCGGCAGATAGCTGGTGG-3'
del1rev	93119 (−)	5'-gcgaattcCTATCGGTACTCCCGGCGATG-3'
del2a	94181 (−)	5'-ggatccactgccggatccactgccCAAAAATAGAGTCGGG-3'
del2b	94086 (+)	5'-ggcagtggatccggcagtggatccAGATATGCCCGGGGG-3'
del3a	94036 (−)	5'-ggatccactgccggatccactgccTGGCCGGGTGCACCC-3'
del3b	93946 (+)	5'-ggcagtggatccggcagtggatccAAGCAGGCAGTCCTGGGG-3'
del4a	94011 (−)	5'-ggatccactgccggatccactgccAACCACGTAAACTGCCG-3'
del4b	93838 (+)	5'-ggcagtggatccggcagtggatccAATCTTCGGATACTAAAGACC-3'
del5−7a	93779 (−)	5'-ggatccactgccggatccactgccGCGTCCGGGTCCG-3'
del5−7b	93505 (+)	5'-ggcagtggatccggcagtggatccTTCCATGCCATGGTTTCC-3'

[a] Numbers represent positions of the primers in the EHV-1 genome, and the strand (+/−) is given. Capital letters indicate gM sequences; lowercase letters indicate restriction enzyme sites or the introduced linker sequence (Gly-Ser)^4. Sequence data are based on Telford et al. (1992).

analysis using lysates prepared from the various cell lines. Mutant gM molecules exhibited sizes after SDS–12% PAGE that were in good agreement with the calculated molecular masses, and oligomerization was clearly detected in RKgMΔ2, RKgMΔ3, and RKgMΔ4 cells (Fig. 5A). However, in lysates of RKgMΔ1 cells, a protein with an apparent M_r of 28,000 was specifically detected with both MAb P1/B6 A8 and the pQEgM antiserum, although an M_r 40,000 protein was expected to be expressed from the gMΔ1 ORF. The M_r 28,000 gM-specific protein was also observed in lysates of cells expressing wild-type or other mutant gM (Figs. 5A, 5B, and Fig. 7). These results indicated either degradation of the mutant gM expressed by RKgMΔ1 or an alternative translation initiation site within the gM ORF. The M_r 28,000 gM-specific band was detected irregularly in cell lines expressing mutant gM, but was constantly, although at varying intensities, detected from 10 h postinfection (p.i.) in lysates of cells infected with wild-type or mutant KyA. In addition, the M_r 28,000 gM-specific band was invariably reduced in size in the case of RKgMΔ5–7 or cells infected with KyAΔgM5–7 (Fig. 7). In contrast, an additional M_r 38,000 gM-specific band was detected only rarely in infected-cell lysates harvested at late times p.i. It was also noted that all investigated cell lines, including RKgM, expressed the high-mannose moiety of the respective glycoprotein only (Fig. 5A). Processing of the various mutant gM glycoproteins was further investigated after infection of mutant cell lines with a gM-negative KyAΔgM (i.e., in the presence of other EHV-1 proteins). As described previously, full-length EHV-1 gM was processed to the mature glycoprotein, and an M_r 50,000–55,000 gM-specific protein was detected with MAb P1/B6 A8 (Fig. 5B) (Osterrieder et al., 1997). In contrast, migration of mutant gM proteins appeared unaltered at 24 h after infection with KyAΔgM, indicating that carbohydrate maturation of
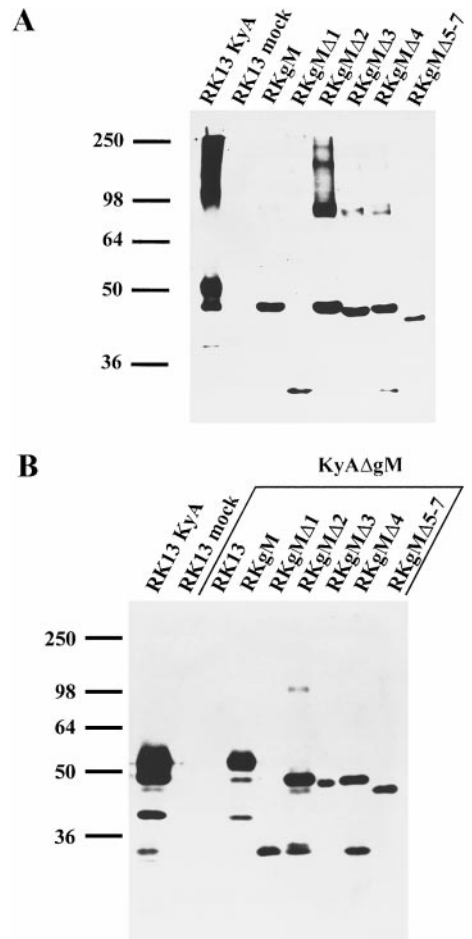

FIG. 5. Western blot analysis of the recombinant cell lines expressing mutant gM. Lysates of recombinant cell lines (A) or recombinant cell lines infected with gM-negative KyAΔgM (B) were separated by SDS–12% PAGE. After transfer to nitrocellulose, sheets were incubated with anti-gM MAb P1/B6 A8. After incubation with anti-mouse IgG peroxidase conjugate (Sigma Chemical Co.), bound antibodies were detected by enhanced chemiluminescence. The positions of molecular weight markers (in thousands) are indicated.

mutant gM proteins in the TGN did not take place (Fig. 5B).

Analysis of recombinant KyA viruses

To analyze the mutant gM proteins in more detail, recombinant KyA viruses that expressed gMΔ2, gMΔ3, gMΔ4, or gMΔ5–7 were constructed. It was impossible to construct a recombinant KyA virus with hydrophobic domain 1 deleted (gMΔ1) because the essential UL9 ORF overlaps that of gM at its 5′-end and deletion of the sequences encoding the first transmembrane domain could abrogate expression of a functional UL9 gene (Malik *et al.,* 1992; Telford *et al.,* 1992). Based on the gM-negative KyAΔgM, the mutated gM genes were inserted into the KyA genome. The respective ORFs were introduced in plasmid pBH3.1 instead of the full-length gM gene (Fig. 1A), and the recombinant plasmids were cotransfected with KyAΔgM DNA into RK13 cells. Transfection progeny was purified until virus populations that produced homogeneously nonfluorescing plaques were obtained. The recombinant viruses were tested by Southern blot analysis for the presence and correct insertion of the mutated gM ORFs (data not shown). RK13 cells were infected with KyAgMΔ2, KyAgMΔ3, KyAgMΔ4, or KyAgMΔ5–7 at an m.o.i. of 2, and at 16 h p.i. infected-cell lysates were harvested and subjected to Western blot analysis. Using MAb P1/B6 A8, gM proteins could be demonstrated in lysates of cells infected with each of the mutants. The respective migration pattern of gM was similar to that of cell lines constitutively expressing mutant gM. Polypeptides of M_r 45,000 (KyAgMΔ2), M_r 43,000 (KyAgMΔ3), M_r 43,000 (KyAgMΔ4), and M_r 41,000 (KyAgMΔ5–7) were specifically detected by the P1/B6 A8 antibody (Fig. 6). In addition, extensive dimerization and oligomerization of mutant gM proteins were observed, although cell lysates were separated in the presence of 2-mercaptoethanol.

Deglycosylation analysis of mutant gM molecules

Enzymatic deglycosylation experiments using lysates of RK13 cells infected with the various mutant viruses were performed to investigate the observed block in maturation of mutant gM polypeptides (Figs. 5B and 6). Although the M_r 50,000–55,000 gM-specific moiety was resistant against treatment with EndoH, all mutant gM proteins proved to be sensitive against EndoH treatment as evidenced by an increased mobility of the various gM-specific proteins after SDS–10% PAGE and immunoblotting using the P1/B6 A8 antibody (Fig. 7). However, all mutant gM proteins entered the endoplasmic reticulum (ER) and were N-glycosylated as demonstrated by sensitivity of the polypeptides against PNGaseF and EndoH (Fig. 7). Thus mutant gM molecules were not correctly processed, and this improper processing was caused by a defect in transport of the molecules through the secre-
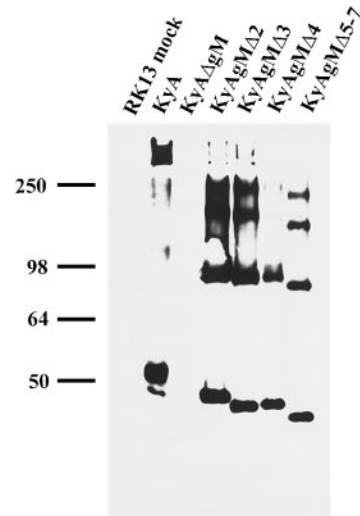

FIG. 6. Western blot analysis of the generated recombinant viruses. Infected cell lysates were harvested at 16 h p.i., separated by SDS–12% PAGE, transferred to nitrocellulose, and incubated with anti-gM MAb P1/B6 A8. After incubation with anti-mouse IgG peroxidase conjugate (Sigma Chemical Co.), bound antibodies were detected by enhanced chemiluminescence. The positions of molecular weight markers (in thousands) are given.

tory pathway to the TGN. Consistent with these findings, none of the mutant gM molecules was incorporated into extracellular virions (data not shown).

Growth of gM-negative and mutant KyA viruses

Plating of KyAΔgM onto RK13 cell lines expressing mutant gM and plating of mutant KyA onto RK13 cells had demonstrated that none of the mutant gM was able to restore plaque sizes to wild-type levels (data not shown). Therefore, in the next series of experiments, single-step growth kinetics were determined. KyAΔgM or KyA expressing the various mutant gM was grown on cells expressing wild-type gM and subsequently used to infect RK13 or RKgM cells at an m.o.i. of 3. The results of these experiments are summarized in Fig. 8. KyAΔgM grown on RK13 cells exhibited a massive reduction in intracellular and especially extracellular virus titers (up to 230-fold) compared with titers of parental KyA (Figs. 8A and 8B). This defect in virus egress was reversed when KyAΔgM was grown on RKgM cells (Figs. 8C and 8D). Infection of RK13 cells with mutant KyAΔgM2, KyAΔgM3, KyAΔgM4, or KyAΔgM5–7 also resulted in intracellular and extracellular virus titers that were reduced up to 600-fold compared with those of wild-type KyA or the rescued KyAΔgM virus (KyAΔgMrev) in which the wild-type gM open reading frame was reinserted (Figs. 8A and 8B). When single-step growth of KyA expressing mutant gM on RKgM was determined, intracellular and extracellular virus titers similar to those of KyAΔgM were observed (Figs. 8C and 8D). From these results, we concluded that efficient growth of EHV-1 in cultured cells
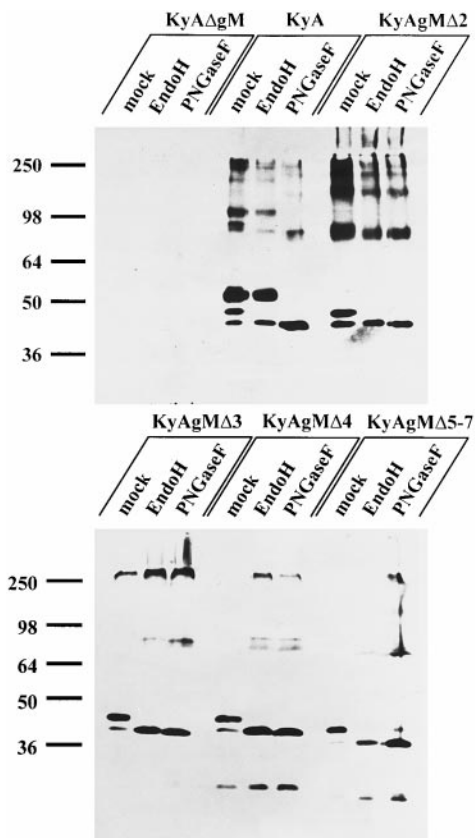
FIG. 7. Deglycosylation of cell lysates infected with the various recombinant viruses. Lysates of infected RK13 cells were digested with PNGaseF or EndoH or were mock-digested. After 16 h of incubation at 37°C, lysates were separated by SDS–10% PAGE, transferred to nitrocellulose, and incubated with anti-gM MAb P1/B6 A8. Bound MAb was detected with anti-mouse IgG peroxidase conjugate (Sigma Chemical Co.) and visualized by enhanced chemiluminescence. The positions of molecular weight markers (in thousands) are given.

requires intact gM and that the deletion of predicted transmembrane domains of gM led to ER retention of gM, which resulted in a massive impairment of cell-to-cell spread and virus egress.

DISCUSSION

The salient findings of the present study are as follows. (1) The simultaneous absence of gE, gI, and gM of EHV-1 led to a massive impairment of virus growth in cultured cells that could be overcome by providing gM *in trans*. (2) The deletion of predicted transmembrane domains of EHV-1 gM resulted in improper processing of the glycoprotein and retention of the molecules in the ER that, as a consequence, were not incorporated into extracellular virions. (3) The retention of mutant gM resulted, at least in a gE/gI-negative virus background, in a small plaque phenotype of mutant viruses and a reduction in both intracellular and extracellular virus titers. These results demonstrate that the absence of transmembrane domains leads to misfolding of gM, which is

consequently absent from TGN membranes and virions. (4) None of the mutant gM proteins exerted a transdominant negative effect on wild-type gM, and recombinant KyA expressing mutant gM exhibited wild-type plaque sizes and virus titers on gM-complementing cells. Similarly, KyA was not impaired in growth on cell lines producing mutant gM proteins lacking individual transmembrane domains.

Several reports have demonstrated that gM and the gE/gI complex are involved in cell-to-cell spread and egress of *Alphaherpesvirinae in vitro* and *in vivo* (Baines and Roizman, 1991, 1993; Balan *et al.,* 1994; Card *et al.,* 1992; Dijkstra *et al.,* 1996; Dingwell *et al.,* 1994, 1995; Enquist *et al.,* 1994; Kimman *et al.,* 1992; Kritas *et al.,* 1994; Matsumura *et al.,* 1996; Mettenleiter *et al.,* 1987; Osterrieder *et al.,* 1996; Zsak *et al.,* 1992). A study demonstrating the functionally concerted action of these three glycoproteins in PrV was performed by Brack *et al.* (1999). It could be shown that simultaneous deletion of gM and gE/gI caused a severe impairment in virus spread and release from infected cells. Based on virus growth characteristics and electron microscopic studies, the authors concluded that both gM and the gE/gI complex are involved in secondary envelopment of virions at Golgi vesicles by mediating interaction of viral envelopes with the tegument. Although the interactions of gM and the gE/gI complex with the tegument occur at different stages and appeared cascade-like, gM can compensate for gE/gI function and gE/gI for gM function to a certain extent. In EHV-1 the situation is similar, and deletion of gM and gE/gI resulted in a drastic reduction in viral cell-to-cell spread and release. This massive impairment in virus growth correlated with an inefficient secondary envelopment at Golgi vesicles as analyzed by electron microscopy, although sequestration of gE/I/M-negative KyA into inclusion bodies as demonstrated for PrV (Brack *et al.,* 1999) could not be observed. However, the rim of fuzzy material that was detected around accumulated KyAΔgM nucleocapsids and was also observed in the case of parental KyA may indicate that inefficient secondary envelopment is not caused by the failure to add tegument proteins to nucleocapsids in the case of gM-negative EHV-1.

Glycoprotein M homologs of herpesviruses are special in several ways. Besides representing multiple hydrophobic proteins encoding eight putative transmembrane domains, gM homologs are conserved throughout the three subfamilies of the *Herpesviridae*. Despite this fact, gM is nonessential for replication of all herpesviruses tested (i.e., virus growth in cultured cells is impaired but still possible in the absence of the protein). After the deletion of gM in HSV-1, PrV, and EHV-1, however, the viruses exhibit reduced virulence or become entirely avirulent in animals (Dijkstra *et al.,* 1997a; MacLean *et al.,* 1993; Neubauer *et al.,* 1997a). In addition, gM forms a complex with the UL49.5 product (gN in PrV and
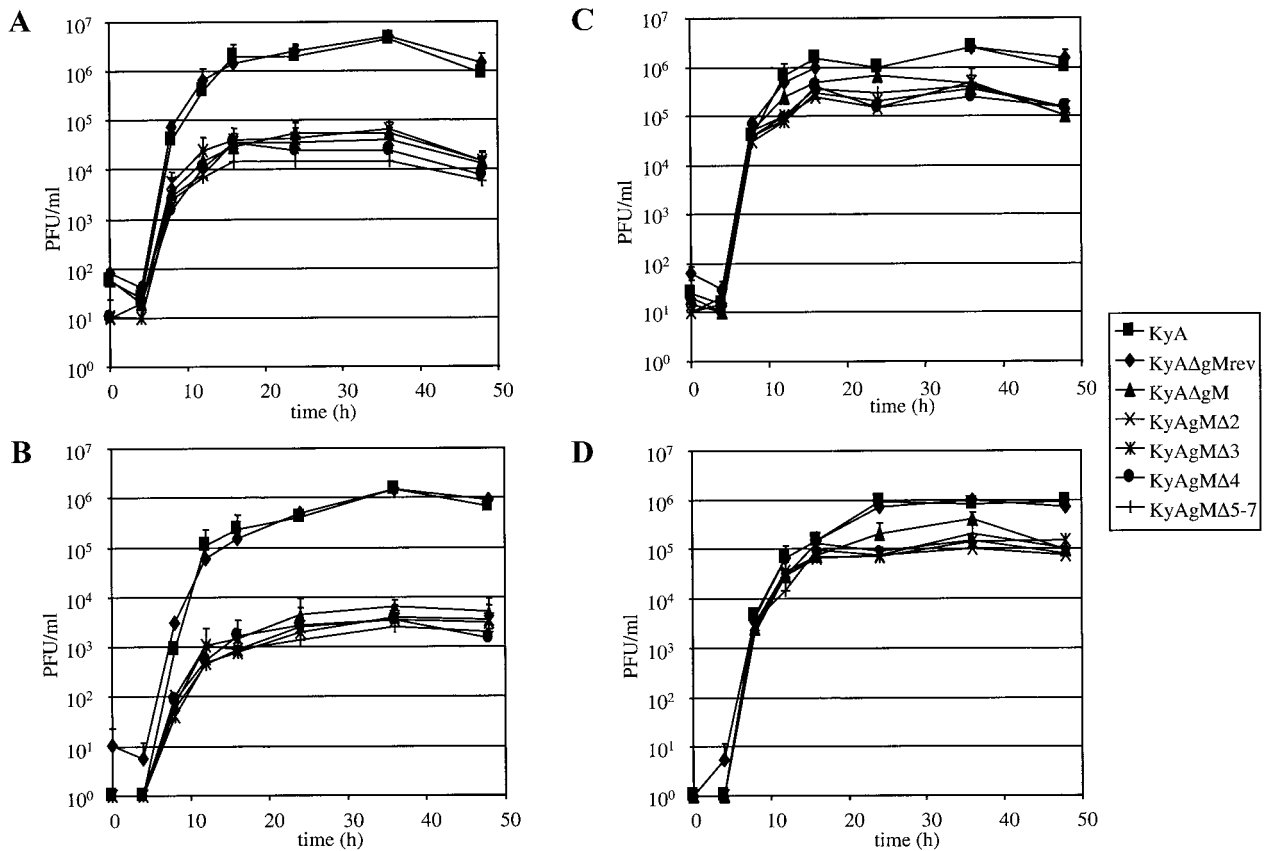
FIG. 8. One-step growth kinetics of the different viruses. RK13 (A, B) or RKgM cells (C, D) were infected with the indicated viruses at an m.o.i. of 3. After adsorption and penetration, supernatants were collected at the indicated times and titrated (B, D). Similarly, infected-cell pellets were harvested and titrated (A, C). The values are means of two independent experiments. Error bars indicate standard deviations.

EBV), although this complex appears to be dispensable for PrV gM processing, for incorporation of gM into virions, and for virus growth *in vitro* and after intranasal injection of mice (Brack *et al.,* 1999; Jöns *et al.,* 1998; Masse *et al.,* 1999). In the case of EBV, gN processing is dependent on coexpression of gM (Lake *et al.,* 1998). For neither of the gM homologs was the function of individual predicted protein domains investigated. In this communication, we demonstrate that gM processing and function are abrogated if the first, second, third, or fourth putative transmembrane domain is deleted. These phenomena were also observed by deletion of the fifth through seventh hydrophobic domains of the glycoprotein, although all mutant proteins entered the ER and carried *N*-glycans. In addition, oligomerization was observed for all mutant gM expressed either constitutively or by mutant viruses. However, it was noted that oligomer formation was much more pronounced after infection with mutant viruses, which may indicate that simultaneous expression of another viral protein or proteins may favor complex formation. It was noted previously that EHV-1 gM was not fully processed in the absence of other viral proteins (Osterrieder *et al.,* 1996, 1997), but in contrast to mutant gM proteins, the EndoH-resistant mature form of the glycoprotein was detectable

in the presence of other viral proteins. The impaired transport of mutant gM molecules lacking an odd number (one or three) of transmembrane domains can be interpreted in several ways, the most likely being misfolding of the protein. Although not formally proved, we hypothesize that mutant gM proteins retain their ability to pass through membranes several times because they still aggregated on heating at 95°C. It must be noted that preliminary data suggest that transport of a mutant gM lacking the third and fourth putative transmembrane domain (i.e., a mutant gM protein with the N terminus of the molecule theoretically present in the cytoplasm as is the case for wild-type gM; Osterrieder *et al.,* 1997) also appeared to be only incompletely processed (C. Seyboldt and N. Osterrieder, unpublished observations). Therefore, further mutant gM with deletions of even numbers of predicted transmembrane domains must be generated to analysis protein processing and a possible restoration of growth of gM-negative KyA.

The presence of an M_r 28,000 gM-specific protein in RKgMΔ1 cells although the expected molecular mass of the gMΔ1 protein was ~40,000 raised the question of whether the M_r 28,000 protein is the result of degradation or of an alternative initiation within the gM ORF. We favor the latter possibility because the M_r 28,000 gM-specific

protein was variably but repeatedly detected in all (mutant) gM cell lines and in cells infected with wild-type KyA or various mutant viruses. In addition, the M_r 28,000 gM-specific band was reduced in size in the case of RKgMΔ5–7 and the corresponding KyA mutant virus but reacted with antibodies directed against the hydrophilic C-terminus of gM. We therefore concluded that the internal translation product is initiated from the methionine codon at position 226 and is terminated at the gM stop codon. This interpretation of an additional ORF is corroborated by the presence of two gM-specific messenger RNAs in several *Alphaherpesvirinae* (Fuchs and Mettenleiter, 1999; Osterrieder, 1999b). In contrast, we view it as likely that the M_r 38,000 polypeptide that was detected with gM antibodies only rarely and at late times p.i. represents a degradation product. Ongoing studies focus on the construction of a set of further mutant gM and corresponding KyA viruses with deletions of an even number of transmembrane and hydrophilic domains. In addition, the nature of the M_r 28,000 and 38,000 gM-specific proteins is currently being addressed by targeted deletions of methionine residues in EHV-1 gM. These studies should shed more light on the topology–function relationship of herpesviral gMs.

MATERIALS AND METHODS

Virus and cells

Strain KyA (kindly provided by Dr. D. J. O'Callaghan, LSUMC, Shreveport, LA) was used in this study. KyA was grown on RK13 cells that were propagated in Dulbecco's minimal essential medium supplemented with 10% FCS. For isolation of a gM-negative KyA, gM-expressing RKgM cell that were generated after transfection of RK13 cells with plasmid pcgM were used exactly as previously described (Osterrieder *et al.,* 1996). pΔgMGFP+ DNA (10 μg) was cotransfected with 1–10 μg of purified KyA DNA into RKgM cells. At 3–5 days after transfection, supernatants were harvested and plated onto fresh RKgM cells. Recombinant fluorescent virus plaques were picked and purified to homogeneity.

Fusion PCR and plasmids

Recombinant plasmid pBH3.1 that contains gM encoding and adjacent sequences (Fig. 1) was digested with *Hinc*II and *Sph*I to remove most of the gM gene, and the green fluorescent protein (GFP) cassette under the control of the human cytomegalovirus immediate-early promoter (pEGFP-N1; Clontech) was inserted (Fig. 1A). The resulting plasmid, pΔgMGFP+, was used to construct gM-negative KyA (KyAΔgM). pBH3.1 was also used for the fusion PCR to obtain gM ORFs with deletions of transmembrane domains. The fusion PCR was composed of two steps (Ho *et al.,* 1989). In the first step, amplicons on either side of the sequence to be deleted

were generated. The internal primers bordering the deletions contained an overlap of 24 nucleotides encoding four Gly-Ser codons (Table 1). In a second step, purified amplicons were subjected to a second round of amplification that was based on the hybridization of overlapping 24 nucleotides and used outer primers only (Fig. 1C). Using this fusion PCR technique, a total of four mutant gM genes that lacked predicted transmembrane domains 2, 3, 4, or 5–7 were constructed (Fig. 1D). Transmembrane domains 5–7 were removed simultaneously because they are only separated by 4 and 9 amino acids, respectively (Telford *et al.,* 1992). For construction of a mutant gM lacking the first transmembrane domain, conventional PCR was done (Table 1, Fig. 1D). Plasmid pQEgM contained amino acids 376–450 of EHV-1 gM (Fig. 1B) fused to a (His)$_6$ tag after cloning of gM sequences in vector pQE30 (Qiagen). After the induction of fusion protein expression, the overexpressed His-tagged protein was electroeluted from a 10% SDS–polyacrylamide gel (BioRad) (Meindl and Osterrieder, 1999).

Generation of cell lines expressing recombinant gM genes

All mutant gM genes were cloned into expression vector pcDNA3 (Invitrogen). Ten micrograms of each of the recombinant plasmids pcgMΔ1, pcgMΔ2, pcgMΔ3, pcgMΔ4, and pcgMΔ5–7 were transfected into RK13 cells, and cell clones developing under medium containing 500 μg/ml G-418 (Calbiochem) were tested for gM expression by indirect immunofluorescence and Western blotting. Positive clones were selected and designated RKgMΔ1, RKgMΔ2, RKgMΔ3, RKgMΔ4, and RKgMΔ5–7, respectively.

Generation of KyA gM recombinants

For construction of KyA expressing mutant gM, plasmids pcgMΔ2, pcgMΔ3, pcgMΔ4, and pcgMΔ5–7 were digested with *Hinc*II and *Sph*I, and the resulting fragments containing the mutant gM sequences were cloned into plasmid pBH3.1 cleaved with the same restriction enzymes (Figs. 1A and 1D). The plasmids were cotransfected with KyAΔgM DNA into RK13 cells. At 3–5 days after transfection, supernatants were harvested and plated onto fresh cells. Recombinant nonfluorescing plaques were picked and purified to homogeneity. The recombinant viruses were termed KyAgMΔ2, KyAgMΔ3, KyAgMΔ4, and KyAgMΔ5–7. A rescuant virus, KyAΔgMrev, was produced after cotransfection of KyAΔgM DNA and plasmid pBH3.1.

Virus penetration assays, single-step growth kinetics, and plaque size determinations

Virus penetration assays were performed essentially as described previously (Osterrieder *et al.,* 1996). The percentage of penetrated virus was calculated according

to the equation % penetration = (number of plaques after pH 3 (sodium citrate) treatment for 1 min)/(number of plaques after treatment with PBS) $\times$ 100. Single-step growth kinetics were determined after infection of 1×10^6 RK13 or RKgM cells at an m.o.i. of 3. Virus was allowed to attach for 2 h on ice, followed by a penetration period of 2 h at 37°C. At the indicated times after the temperature shift, supernatants of infected cells and infected cell pellets were harvested, and viral titers were determined by plating onto RK13 cells. Plaque sizes were measured after titration of virus mutants on different cell lines and 3 days of incubation at 37°C under a methylcellulose overlay. Cells were fixed with 5% formaldehyde and stained with crystal violet. For each combination of virus and cell, 150 plaques were measured and the average plaque sizes were determined. Values were calculated and compared with KyA plaque sizes, which were set to 100%. Average percentages of plaque sizes and standard deviations were determined from three independent experiments.

Electron microscopy

For ultrastructural analyses, RK13 cells were infected at an m.o.i. of 1 and fixed at different times p.i. (16–20 h) for 60 min with 2.5% glutaraldehyde buffered in 0.1 M Na cacodylate [pH 7.2, 300 mOsmol (Merck, Darmstadt, Germany)]. Cells were then scraped off the flask, pelleted by low-speed centrifugation, and embedded in LMP agarose (Biozym). Small pieces were postfixed in 1.0% aqueous OsO_4 (Polysciences Europe) and stained with uranyl acetate. After stepwise dehydration in ethanol, cells were cleared in propylene oxide, embedded in Glycid Ether 100 (Serva, Heidelberg, Germany), and polymerized at 59°C for 4 days. Ultrathin sections were counterstained with uranyl acetate and lead salts and examined by electron microscopy (Siemens Elmiskop 101 and Philips EM 400T).

Antibodies

Anti-EHV-1 MAbs directed against gM were kindly provided by Drs. Lindsey Day and Richard Killington (University of Leeds, UK) (Day, 1999). A polyclonal rabbit anti-gM antiserum was produced after injection of the pQEgM protein suspended in Freund's complete (first immunization) or incomplete adjuvant (booster immunizations) for a total of five times into a New Zealand White rabbit (Charles River).

Indirect immunofluorescence and Western blotting

For IIF, cells were grown on glass coverslips and subsequently infected at an m.o.i. of 0.01. Cells were fixed with acetone at 48 h p.i., and IIF was done exactly as described (Meindl and Osterrieder, 1999). Samples were analyzed by confocal laser scanning microscopy (Osterrieder *et al.,* 1998; Meindl and Osterrieder, 1999).

For Western blot analyses, RK13 cells were infected at an m.o.i. of 2 with the different viruses. At 16 h after infection, cell lysates were prepared and adjusted to equal protein concentrations of 5 mg/ml as determined by the BCA kit (Pierce Chemical Co.) (Osterrieder *et al.,* 1997). Samples were separated by SDS–PAGE. After separation, proteins were transferred to nitrocellulose membranes (Schleicher & Schüll) by the semidry method (Kyhse-Andersen, 1984). Free binding sites on the sheets were blocked by the addition of 10% skim milk in PBS containing 0.05% Tween (PBST) before the antibodies (suspended in PBST) were added. Bound antibodies were detected with anti-rabbit (-mouse) immunoglobulin G (IgG) peroxidase conjugates (Sigma Chemical Co.) and visualized by enhanced chemiluminescence (ECL; Pharmacia-Amersham).

Deglycosylation of cell lysates

Deglycosylation experiments were performed by suspending infected-cell lysates (from 1×10^6 cells) in 100 μl deglycosylation buffer (50 mM K_3PO_4, pH 7.2, 50 mM EDTA, 0.6% v/v CHAPS, 0.1% SDS) and the subsequent addition of PNGaseF (0.4 U) or EndoH (2 mU) (Roche Biochemicals). Control lysates were left untreated. After 16 h of incubation at 37°C, lysates were separated by 10% SDS–PAGE, transferred to nitrocellulose, and examined by Western blotting.

REFERENCES

Allen, G. P., and Bryans, J. T. (1986). Molecular epizootiology, pathogenesis, and prophylaxis of equine herpesvirus-1 infections. *Prog. Vet. Microbiol. Immunol.* **2,** 78–144.

Allen, G. P., and Yeargan, M. R. (1987). Use of λgt11 and monoclonal antibodies to map the genes for the six major glycoproteins of equine herpesvirus 1. *J. Virol.* **61,** 2454–2461.

Baines, J. D., and Roizman, B. (1991). The open reading frames UL3, UL4, UL10, and UL16 are dispensable for the replication of herpes simplex virus 1 in cell culture. *J. Virol.* **65,** 938–944.

Baines, J. D., and Roizman, B. (1993). The UL10 gene of herpes simplex virus 1 encodes a novel viral glycoprotein, gM, which is present in the virion and in the plasma membrane of infected cells. *J. Virol.* **67,** 1441–1452.

Balan, P., Davis-Poynter, N., Bell, S., Atkinson, H., Browne, H., and Minson, T. (1994). An analysis of the in vitro and in vivo phenotypes of mutants of herpes simplex virus type 1 lacking glycoproteins gG, gE, gI or the putative gJ. *J. Gen. Virol.* **75,** 1245–1258.

Brack, A. R., Dijkstra, J. M., Granzow, H., Klupp, B. G., and Mettenleiter, T. C. (1999). Inhibition of virion maturation by simultaneous deletion of glycoproteins E, I, and M of pseudorabies virus. *J. Virol.* **73,** 5364–5372.

Card, J. P., Whealy, M. E., Robbins, A. K., and Enquist, L. W. (1992).

Pseudorabies virus envelope glycoprotein gI influences both neurotropism and virulence during infection of the rat visual system. *J. Virol.* **66,** 3032–3041.

Colle, C. F., Flowers, C. C., and O'Callaghan, D. J. (1992). Open reading frames encoding a protein kinase, homolog of glycoprotein gX of pseudorabies virus, and a novel glycoprotein map within the unique short segment of equine herpesvirus type 1. *Virology* **188,** 545–557.

Crabb, B. S., Nagesha, H. S., and Studdert, M. J. (1992). Identification of equine herpesvirus 4 glycoprotein G: A type-specific, secreted glycoprotein. *Virology* **190,** 143–154.

Csellner, H., Wellington, J. E., Walker, C., McLure, L. E., Love, D. N., and Whalley, J. M. (1999). EHV-1 gD is essential for virus entry and cell-to-cell spread, and a gD deletion mutant induces a protective immune response in mice. Abstr. 24th International Herpesvirus Workshop.

Day, L. (1999). Characterisation of selected glycoproteins of equine herpesvirus-1: Immune responses in the murine model. Ph.D. thesis, University of Leeds, UK.

Dijkstra, J. M., Gerdts, V., Klupp, B. G., and Mettenleiter, T. C. (1997). Deletion of glyco-protein gM of pseudorabies virus results in attenuation for the natural host. *J. Gen. Virol.* **78,** 2147–2151.

Dijkstra, J. M., Mettenleiter, T. C., and Klupp, B. G. (1997). Intracellular processing of pseudorabies virus glycoprotein M (gM): gM of strain Bartha lacks N-glycosylation. *Virology* **237,** 113–122.

Dijkstra, J. M., Visser, N., Mettenleiter, T. C., and Klupp, B. G. (1996). Identification and characterization of pseudorabies virus glycoprotein gM as a nonessential virion component. *J. Virol.* **70,** 5684–5688.

Dingwell, K. S., Brunetti, C. R., Hendricks, R. L., Tang, Q., Tang, M., Rainbow, A. J., and Johnson, D. C. (1994). Herpes simplex virus glycoproteins E and I facilitate cell-to-cell spread in vivo and across junctions of cultured cells. *J. Virol.* **68,** 834–845.

Dingwell, K. S., Doering, L. C., and Johnson, D. C. (1995). Glycoproteins E and I facilitate neuron-to-neuron spread of herpes simplex virus. *J. Virol.* **69,** 7087–7098.

Enquist, L. W., Dubin, J., Whealy, M. E., and Card, J. P. (1994). Complementation analysis of pseudorabies virus gE and gI mutants in retinal ganglion cell neurotropism. *J. Virol.* **68,** 5275–5279.

Flowers, C. C., and O'Callaghan, D. J. (1992). The equine herpesvirus type 1 (EHV-1) homolog of herpes simplex virus type 1 US9 and the nature of a major deletion within the unique short segment of the EHV-1 KyA strain genome. *Virology* **190,** 307–315.

Fuchs, W., and Mettenleiter, T. C. (1999). DNA sequence of the UL6 to UL20 genes of infectious laryngotracheitis virus and characterization of the UL10 gene product as a nonglycosylated and nonessential virion protein. *J. Gen. Virol.* **80,** 2173–2182.

Granzow, H, Weiland, F., Jöns, A., Klupp, B. G., Karger, A., and Mettenleiter, T. C. (1997). Ultrastructural analysis of the replication cycle of pseudorabies virus in cell culture: A reassessment. *J. Virol.* **71,** 2072–82.

Ho, S. N., Hunt, H. D., Horton, R. M., Pullen, J. K., and Pease, L. R. (1989). Site-directed mutagenesis by overlap extension using the polymerase chain reaction. *Gene* **77,** 51–59.

Jöns, A., Dijkstra, J. M., and Mettenleiter, T. C. (1998). Glycoproteins M and N of pseudorabies virus form a disulfide-linked complex. *J. Virol.* **72,** 550–557.

Kimman, T. G., de Wind, N., Oei-Lie, N., Pol, J. M., Berns, A. J., and Gielkens, A. L. (1992). Contribution of single genes within the unique short region of Aujeszky's disease virus (suid herpesvirus type 1) to virulence, pathogenesis and immunogenicity. *J. Gen. Virol.* **73,** 243–251.

Kritas, S. K., Pensaert M. B., and Mettenleiter, T. C. (1994). Role of envelope glycoproteins gI, gp63 and gIII in the invasion and spread of Aujeszky's disease virus in the olfactory nervous pathway of the pig. *J. Gen. Virol.* **75,** 2319–2327.

Kyhse-Andersen, J. (1984). Electroblotting of multiple gels: A simple apparatus without buffer tank for rapid transfer of proteins from polyacrylamide to nitrocellulose. *J. Biochem. Biophys. Methods* **10,** 203–209.

Lake, C. M., Molesworth, S. J., and Hutt-Fletcher, L. M. (1998). The Epstein-Barr virus (EBV) gN homolog BLRF1 encodes a 15-kilodalton glycoprotein that cannot be authentically processed unless it is coexpressed with the EBV gM homolog BBRF3. *J. Virol.* **72,** 5559–5564.

MacLean, C. A., Robertson, L. M., and Jamieson, F. E. (1993). Characterization of the UL10 gene product of herpes simplex virus type 1 and investigation of its role in vivo. *J. Gen. Virol.* **74,** 975–983.

Malik, A. K., Martinez, R., Muncy, L., Carmichael, E. P., and Weller, S. K. (1992). Genetic analysis of the herpes simplex virus type 1 UL9 gene: Isolation of a LacZ insertion mutant and expression in eukaryotic cells. *Virology* **190,** 702–715.

Masse, M. J., Jöns, A., Dijkstra, J. M., Mettenleiter, T. C., and Flamand, A. (1999). Glycoproteins gM and gN of pseudorabies virus are dispensable for viral penetration and propagation in the nervous systems of adult mice. *J. Virol.* **73,** 10503–10507.

Matsumura, T., Kondo, T., Sugita, S., Damiani, A. M., O'Callaghan, D. J., and Imagawa, H. (1998). An equine herpesvirus type 1 recombinant with a deletion in the gE and gI genes is avirulent in young horses. *Virology* **242,** 68–79.

Matsumura, T., O'Callaghan D. J., Kondo, T., and Kamada, M. (1996). Lack of virulence of the murine fibroblast adapted strain, Kentucky A (KyA), of equine herpesvirus type 1 (EHV-1) in young horses. *Vet. Microbiol.* **48,** 353–365.

Meindl, A., and Osterrieder, N. (1999). The equine herpesvirus 1 Us2 homolog encodes a nonessential membrane-associated virion component. *J. Virol.* **73,** 3430–3437.

Mettenleiter, T. C., Schreurs, C., Zuckermann, F., and Ben-Porat, T. (1987). Role of pseudorabies virus glycoprotein gI in virus release from infected cells. *J. Virol.* **61,** 2764–2769.

Neubauer, A., Beer, M., Brandmüller, C., Kaaden, O.-R., and Osterrieder, N. (1997a). Equine herpesvirus 1 mutants devoid of glycoprotein B or M are apathogenic for mice but induce protection against challenge infection. *Virology* **239,** 36–45.

Neubauer, A., Braun, B., Brandmüller, C., Kaaden, O.-R., and Osterrieder, N. (1997b). Analysis of the contributions of the equine herpesvirus 1 glycoprotein gB homolog to virus entry and direct cell-to-cell spread. *Virology* **227,** 281–294.

O'Callaghan, D. J., and Osterrieder, N. (1999). The equine herpesviruses. *In* "Encyclopedia of Virology," 2nd ed. (A. Granoff and R. G. Webster, Eds.). Academic Press, Orlando, FL.

Osterrieder, N. (1999a). Construction and characterization of an equine herpesvirus 1 glycoprotein C negative mutant. *Virus Res.* **59,** 165–177.

Osterrieder, N. (1999b). Sequence and initial characterization of the U(L)10 (glycoprotein M) and U(L)11 homologous genes of serotype 1 Marek's disease virus. *Arch. Virol.* **144,** 1853–1863.

Osterrieder, N., Neubauer, A., Brandmüller, C., Braun, B., Kaaden, O.-R., and Baines, J. D. (1996). The equine herpesvirus 1 glycoprotein gp21/22a, the herpes simplex virus type 1 gM homolog, is involved in virus penetration and cell-to-cell spread of virions. *J. Virol.* **70,** 4110–4115.

Osterrieder, N., Neubauer, A., Brandmüller, C., Kaaden, O.-R., and O'Callaghan, D. J. (1998). The equine herpesvirus 1 IR6 protein that colocalizes with nuclear lamins is involved in nucleocapsid egress and migrates from cell to cell independently of virus infection. *J. Virol.* **72,** 9806–9817.

Osterrieder, N., Neubauer, A., Fakler, B., Brandmüller, C., Seyboldt, C., Kaaden, O.-R., and Baines, J. D. (1997). Synthesis and processing of the equine herpesvirus 1 glycoprotein M. *Virology* **232,** 230–239.

Pilling, A., Davison, A. J., Telford, E. A., and Meredith, D. M. (1994). The equine herpesvirus type 1 glycoprotein homologous to herpes simplex virus type 1 glycoprotein M is a major constituent of the virus particle. *J. Gen. Virol.* **75,** 439–442.

Stokes, A., Alber, D. G., Greensill, J., Amellal, B., Carvalho, R., Taylor, L. A., Doel, T. R., Killington, R. A., Halliburton, I. W., and Meredith,

D. M. (1996). The expression of the proteins of equine herpesvirus 1 which share homology with herpes simplex virus 1 glycoproteins H and L. *Virus Res.* **40,** 91–107.

Sullivan, D. C., Allen, G. P., and O'Callaghan, D. J. (1989). Synthesis and processing of equine herpesvirus type 1 glycoprotein 14. *Virology* **173,** 638–646.

Telford, E. A., Watson, M. S., McBride, K., and Davison, A. J. (1992). The DNA sequence of equine herpesvirus-1. *Virology* **189,** 304–316.

Wu, S. X., Zhu, X. P., and Letchworth, G. J. (1998). Bovine herpesvirus 1 glycoprotein M forms a disulfide-linked heterodimer with the U_L 49.5 protein. *J. Virol* **72,** 3029–3036.

Zhao, Y., Holden, V. R., Harty, R. N., and O'Callaghan D. J. (1992). Identification and transcriptional analyses of the UL3 and UL4 genes of equine herpesvirus 1, homologs of the ICP27 and glycoprotein K genes of herpes simplex virus. *J. Virol.* **66,** 5363–5372.

Zsak, L., Zuckermann, F., Sugg, N., and Ben-Porat, T. (1992). Glycoprotein gI of pseudorabies virus promotes cell fusion and virus spread via direct cell-to-cell transmission. *J. Virol.* **66,** 2316–2325.